NANO LETTERS
Letter
Cite This: Nano Lett. 2019, 19, 5836−5843
pubs.acs.org/NanoLett

Ionic Liquid Gated Carbon Nanotube Saturable Absorber for Switchable Pulse Generation

Yuriy Gladush,*[,†] Aram A. Mkrtchyan,[†,‡] Daria S. Kopylova,[†] Aleksey Ivanenko,[§] Boris Nyushkov,[§,∥] Sergey Kobtsev,[§] Alexey Kokhanovskiy,[§] Alexander Khegai,[⊥] Mikhail Melkumov,[⊥] Maria Burdanova,[#] Michael Staniforth,[#] James Lloyd-Hughes,[#] and Albert G. Nasibulin*[,†,▽]

[†]Skolkovo Institute of Science and Technology, Moscow 121205, Russia
[‡]Moscow Institute of Physics and Technology, Moscow region, Dolgoprudny 141700, Russia
[§]Novosibirsk State University, Novosibirsk 630090, Russia
[∥]Novosibirsk State Technical University, Novosibirsk 630073, Russia
[⊥]Fiber Optic Research Center, Moscow 119333, Russia
[#]Department of Physics, University of Warwick, Coventry CV4 7AL, United Kingdom
[▽]Department of Applied Physics and Department of Chemistry and Materials Science, Aalto University, FI-00076 Aalto, Espoo, Finland

Supporting Information

ABSTRACT: Materials with electrically tunable optical properties offer a wide range of opportunities for photonic applications. The optical properties of the single-walled carbon nanotubes (SWCNTs) can be significantly altered in the near-infrared region by means of electrochemical doping. The states' filling, which is responsible for the optical absorption suppression under doping, also alters the nonlinear optical response of the material. Here, for the first time we report that the electrochemical doping can tailor the nonlinear optical absorption of SWCNT films and demonstrate its application to control pulsed fiber laser generation. With a pump−probe technique, we show that under an applied voltage below 2 V the photobleaching of the material can be gradually reduced and even turned to photoinduced absorption. Furthermore, we integrated a carbon nanotube electrochemical cell on a side-polished fiber to tune the absorption saturation and implemented it into the fully polarization-maintaining fiber laser. We show that the pulse generation regime can be reversibly switched between femtosecond mode-locking and microsecond Q-switching using different gate voltages. This approach paves the road toward carbon nanotube optical devices with tunable nonlinearity.

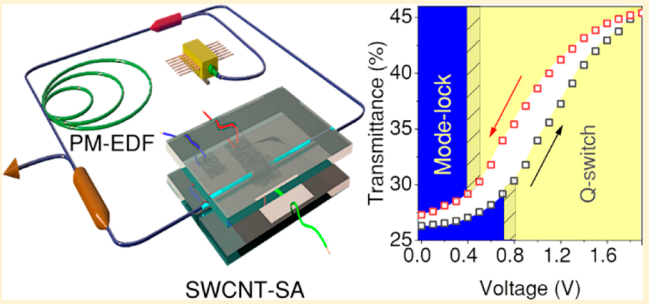

KEYWORDS: *Carbon nanotubes, electrochemical gating, nonlinear optics, saturable absorption, ionic liquid, fiber lasers*

Single-walled carbon nanotubes (SWCNTs) is one of the unique materials in which all atoms are located on the surface. This provides a simple opportunity to manipulate their electronic structure. Unlike bulk materials, to dope SWCNTs it is not necessary to substitute carbon atoms in the lattice by a dopant. Instead, the dopant can be accommodated on the nanotube surface (adsorption doping), inducing electron transfer between the nanotube and the dopant.[1] An excess charge in the nanotubes results in the shift of the Fermi level, greatly altering their optoelectronic properties. It greatly increases the conductivity of SWCNTs,[2] but also allows control of its optical properties[3] by suppressing the near-infrared absorption corresponding to interband excitonic transitions.

Another alternative for Fermi level tuning is electrochemical doping, also referred to as electrochemical gating.[4,5] In this case, the excess charge is formed on the surface of SWCNTs in an electrolyte when an external electric potential is applied. It leads to the formation of an electrical double layer, which can be understood as a capacitor with subnanometer gap formed by charge carriers on the SWCNT side and ions on the electrolyte side.[6] This type of doping has great advantages when high doping level, controllability, and reversibility are required. In fundamental research, electrochemical gating has been used to investigate the formation of trions and other quasiparticles[7−9] and the buildup of the plasmonic response.[10−12] It is also of potential interest for the development of electrochromic devices like smart windows, notch filters, and

Received: March 11, 2019
Revised: July 12, 2019
Published: July 25, 2019

DOI: 10.1021/acs.nanolett.9b01012
Nano Lett. 2019, 19, 5836−5843

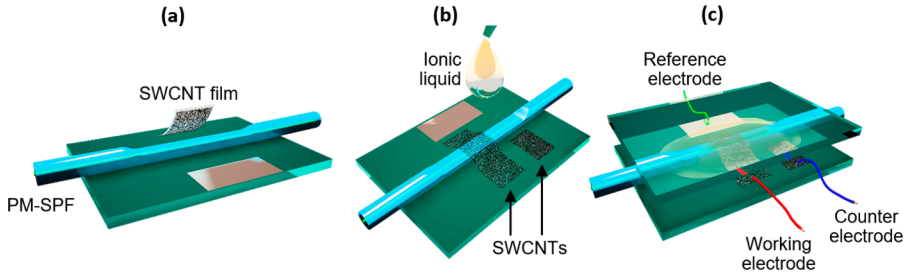

Figure 1. Sample fabrication steps. (a) Reference silver electrode is deposited on the cover glass; side-polished fiber is fixed on the cover glass with deposited silver electrode; SWCNT are dry-transferred on the side polished fiber to form a saturable absorber and electrodes; (b) ionic liquid is dripped on the sample to cover all three electrodes; (c) sample is covered by another cover glass from the top and sealed from the air.

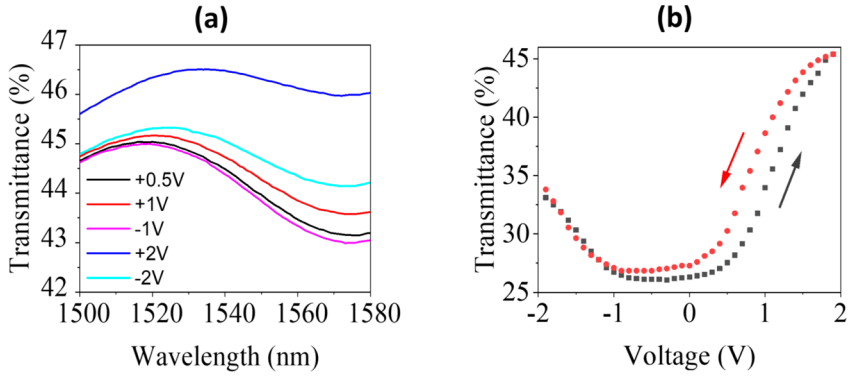

Figure 2. Transmittance of the gated SWCNTs for (a) normal incident light through a 40 nm film, and (b) through the fast axis of PM-SPF device measured with PM ASE source (1530−1570 nm).

modulators.[13−16] The above-mentioned investigations address only the linear optical response of electrochemically gated carbon nanotubes. Carbon nanotubes also show a prominent nonlinear optical response including optical limiting,[17−19] harmonic generation,[20,21] four-wave mixing,[22−25] and absorption saturation.[26−29] The latter one has been a subject of intense investigation for the past decade due to the successful integration of carbon nanotube saturable absorbers (SWCNT-SA) into fiber lasers for noise filtering and ultrashort pulse generation.[30−34] The linear optical absorption modulation by means of the gating can be utilized in fiber laser for active driving of pulse generation.[35,36] The prominent effect that electrochemical gating has on the linear optical properties should also be substantial for nonlinear optical response.[37−40] The filling of states, produced by the Fermi level shift, is expected to modify the conditions for resonant nonlinearities. It opens up possibilities for the development of electrically tunable SWCNT-based nonlinear optical devices.

In the present work, for the first time we demonstrate SWCNT devices with nonlinear optical response controlled by electrochemical doping. We focus on the effect of saturable absorption and its application in fiber lasers. Ionic liquid gating allows us to tune the Fermi level position and reduce the absorption associated with the S_{11} transition and notably change its nonlinear optical response. We use a pump−probe technique to retrieve the main parameters of the gated SWCNTs such as a relative saturation depth and relaxation time. Next, we fabricate a gated carbon nanotube saturable absorber on the polarization-maintaining side-polished fiber (PM-SPF) for in-line implementation in the fiber laser system. With this device, we demonstrate a universal pulsed laser, which is able to operate in mode-locked and Q-switched regimes controlled by the gate voltage. A laser is built with polarization-maintaining (PM) components to avoid the effect of nonlinear polarization evolution[41] and, thus, to ensure the stable and reproducible operation exclusively driven by the SWCNT-SA.

The SWCNTs were synthesized by the aerosol (floating catalyst) chemical vapor deposition method.[42] The SWCNTs were grown on aerosol catalyst particles in the hot reactor zone in a CO atmosphere. At the outlet of the reactor, the SWCNTs were collected on a filter and formed a film of randomly oriented networks of semiconducting and metallic nanotubes. The mean diameter of the SWCNTs was adjusted to synthesize the tubes so that the peak of S_{11} absorbance matched with the erbium laser's gain spectra.[43] The thickness of the film was controlled by the collection time.[44] The transmittance and Raman spectra of as-synthesized SWCNTs can be found in Supporting Information, Figure S2.

The samples were prepared using a dry transfer technique: the collected film on the filter was pressed against the desired surface and therefore transferred the tubes to the substrate.[45] No purification, sonication, or any other liquid chemistry steps were involved in the fabrication of the SWCNT films.

The sample for the fiber laser had a three-electrode configuration with working and counter electrodes made of the SWCNTs and a silver electrode used as a reference. The device was made in three steps, depicted in Figure 1. First, a SWCNT film was dry-transferred from the filter onto the PM-SPF surface and glass substrate. Another SWCNT film was transferred in a close proximity for a counter electrode. Then ionic liquid was cast on the sample to interpenetrate the SWCNTs and cover all three electrodes. The sample was enclosed by a coverslip to protect the ionic liquid from environmental degradation. For the pump−probe spectroscopy measurements at normal light incidence, the sample was

DOI: 10.1021/acs.nanolett.9b01012
Nano Lett. 2019, 19, 5836−5843

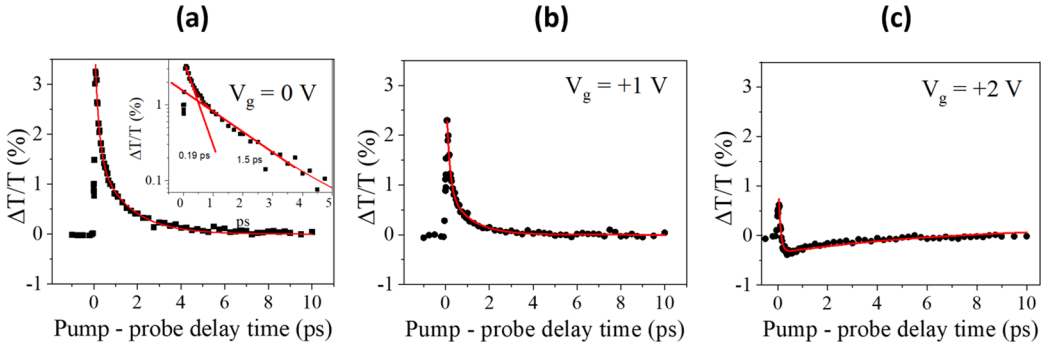

Figure 3. Pump−probe spectroscopy of a gated SWCNT-SA thin film at normal incidence at 1540 nm probe and pump under (a) 0 V, (b) + 1 V, and (c) + 2 V. The inset in the first panel shows the same graph in log scale.

prepared in a similar scheme but without PM-SPF (see Materials and Methods).

First, we measured the transmittance spectra of the samples under gating when the SWCNTs were illuminated with a normally incident beam. To determine the electrochemical stability window for our sample we performed cyclic voltammetry measurements that revealed stable and reproducible behavior for scanning range between −2 and +2 V (see Figure S1 in Supporting Information). The SWCNT transmittance spectrum corresponding to the S_{11} transition under gating is shown in Figure 2a. As the voltage was increased toward +2 V or −2 V, the transmission increased because the S_{11} absorption was lowered by conduction band filling or valence band depletion. A similar behavior is observed for the transmittance of light through the PM-SPF. The transmittance through the fast axis (polarization parallel to the polished surface) of a PM-SPF as a function of voltage measured with a PM C-band ASE source (1530−1570 nm) is shown in Figure 2b. The nanotubes are randomly oriented, but mostly in the plane of the surface of the polished fiber, so this polarization ensures maximum SWCNT−light interaction. An observed hysteresis behavior is typical for electrochemical doping and can be explained by a difference in the potential required for ions to enter the double layer region or to leave it.[16] Both samples demonstrate a negative shift of the transmittance minimum most likely due to the environmental doping.

To investigate the nonlinear optical response of the gated sample, we used degenerate pump−probe spectroscopy and measured the dynamics of absorption saturation and its recovery time. Here, we utilized the gated thin-film sample without the fiber, working at normal incidence in the transmission geometry. An amplified Ti:sapphire laser provided 40 fs pulses, which pumped an optical parametric amplifier to output pulses at 1540 nm with working spectral width of 50 nm. The pump and probe fluences were 382 and 159 $\mu J/cm^2$, respectively. This energy was high enough to ensure absorption saturation and not to burn the SWCNT film. Figure 3 shows the pump-induced differential transmission dynamics, $\Delta T/T(t)$, within a 1.3 nm window around 1540 nm, where a positive sign corresponds to the photobleaching of the sample. We did not find significant dynamic variation across the available spectral window. At zero pump−probe delay time, a large positive $\Delta T/T$ can be seen. This photobleaching signal gives the modulation depth of the absorption saturation. It is always observed around S_{11} in the pump−probe studies of carbon nanotubes as a result of the pump depleting the ground state, lowering the absorption of the probe.[27,46] For our samples, the observed transient transmission change can be fit by the sum of two exponential decays: $\Delta T/T = A_1 e^{-t/\tau_1} + A_2 e^{-t/\tau_2}$. For the undoped sample, the shorter time constant was $\tau_1 = 0.19 \pm 0.01$ ps and the slower decay had $\tau_2 = 1.5 \pm 0.1$ ps. The ratio between the amplitudes of the fast and slow decays was $A_1/A_2 = 1.7 \pm 0.1$, and thus the faster decay had a larger overall contribution to the relaxation dynamics. With a small shift in the chemical potential (V_g = 1 V), $\Delta T/T$ was reduced in the amplitude whereas the dynamics became faster with both time constants shortening ($\tau_1 = 0.14 \pm 0.02$ ps, $\tau_2 = 1.0 \pm 0.2$ ps) and with a relatively greater contribution from the faster decay ($A_1/A_2 = 2.5 \pm 0.5$). The reduced amplitude cannot be fully described by the reduced absorption (the transmittance increases) of the pump beam under gating and attributed to the upper state partial filling when the chemical potential is higher. A faster decay can result from the increased Auger recombination rate in the doped samples.[47] With a higher applied bias voltage, the initial positive peak in $\Delta T/T$ is further reduced (Figure 3c), and $\Delta T/T$ changes the sign. This behavior can be reproduced by a fast decay ($\tau_1 = 0.08 \pm 0.01$ ps) with positive A_1, and a slower decay ($\tau_2 = 7.1 \pm 0.5$ ps) with a negative sign, such that $A_1/A_2 = -3.6 \pm 0.5$. The negative $\Delta T/T$ component may result from an intraband transition, either associated with intersubband plasmon absorption[12] or with the tail of intraband absorption from axial plasmons,[10] which peaks in the far-infrared but which extends throughout the infrared region.

The dynamical response of the SWCNT-SA structure is therefore below one picosecond, in favor of ultrashort pulse generation. At all applied voltages, the SWCNT-SA functions as a saturable absorber with a transient photobleaching showing subpicosecond dynamics. The maximum modulation depth is reduced with higher applied voltages: at zero volts $\Delta T/T$ = 3.2%, whereas $\Delta T/T$ = 2.3% at +1 V and $\Delta T/T$ = 0.7% at +2 V. Therefore, under an applied voltage the saturable absorption of the SWCNT can be readily tuned.

The modulation depth, relaxation time, and saturation fluence are the main parameters governing saturable absorber performance in a fiber laser for a pulse generation either for passive mode-locking (ML), Q-switching (QS), or Q-switched mode-locking. It was suggested theoretically[48−50] and shown experimentally[37,51] for fiber laser systems that by adjusting saturable absorber modulation depth one can change the condition for gain oscillation and switch between different pulse generation regimes.

To demonstrate the switchable pulse generation with a tunable gated SWCNT-SA, we integrated it into an erbium-based fiber laser. First, we tested our samples in a fiber laser

DOI: 10.1021/acs.nanolett.9b01012
Nano Lett. 2019, 19, 5836−5843

without polarization maintaining. We observed the pulse regime switching by the gate voltage, however, the behavior of the laser system was not quite reproducible. We attribute this behavior to the contribution of nonlinear polarization evolution that comes from the polarization dependent loss in SPF sample[52] (see Supporting Information for details). Here we describe instead a laser that featured an all-polarization-maintaining ring cavity design (Figure 4). This all-PM cavity

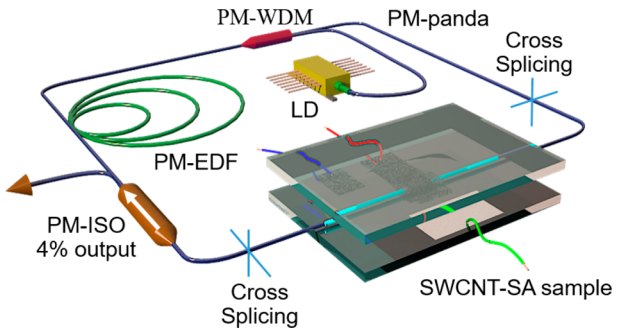

Figure 4. All-PM Er-fiber laser with the gated SWCNT-SA.

design ensured environmentally stable SWCNT-SA-driven pulse generation not affected by nonlinear polarization evolution. A polarization-maintaining erbium-doped fiber (PM-EDF) served as the gain medium of the laser. We used 0.6 m of heavily doped PM-EDF (Nufern PM-ESF-7/125) with anomalous dispersion at the lasing wavelength. The active fiber was pumped by a laser diode (LD) at 980 nm through a polarization-maintaining wavelength division multiplexer (PM-WDM). To keep unidirectional lasing, we also placed a polarization-maintaining optical isolator (PM-ISO) into the cavity. This PM-ISO had an integrated 4% fiber-coupled tap output that allowed extraction of the laser radiation from the cavity. The lasing and pumping waves were counter-propagating in the cavity. The sample of gated SWCNT-SA for the pulsed lasing was prepared with the use of PM-SPF where the polished side was perpendicular to the slow axis plane of the original PM fiber. Therefore, PM fiber pigtails of the sample were connected with the corresponding PM fibers of the laser cavity in the cross-splicing manner (slow axes of the connected fibers were mutually perpendicular). Such a fiber arrangement ensured that the polarization plane of the laser radiation was parallel to the polished side in the sample which maximizes the absorption and thus provides maximum modulation depth. The full length of the fiber resonator was about 4.1 m and the net dispersion was approximately −0.09 ps^2. The all-anomalous dispersion of the laser cavity fulfills the key condition for soliton pulse shaping in mode-locked generation regimes.[53]

First of all, the laser was examined under zero gate voltage. Continuous wave (CW) generation started at 20 mW of the pump power. Mode locking self-starting occurred when the pump power was increased up to 40 mW. Stable ML lasing at the fundamental pulse repetition rate of 50 MHz could be maintained continuously unless the pump power exceeded 95 mW. At a higher pump level, the laser switched over to multipulse lasing that could be attributed to harmonic mode locking (HML). We measured the basic laser characteristics in the single-pulse ML regime sustained at a pump power of 90 mW. The acquired optical spectrum, intensity autocorrelation function, oscillogram, and radiofrequency spectrum of the pulse train are shown in Figure 5a–c and Figure S3a. The spectrum width at half-maximum is 7.6 nm which corresponds to 0.34 ps pulse width assuming the transform-limited $sech^2$ pulse envelope. The measured autocorrelation function corresponds to the 0.6 ps pulse width which is almost twice as long compared to the transform-limited one because the pulse has propagated through the amplifier prior to

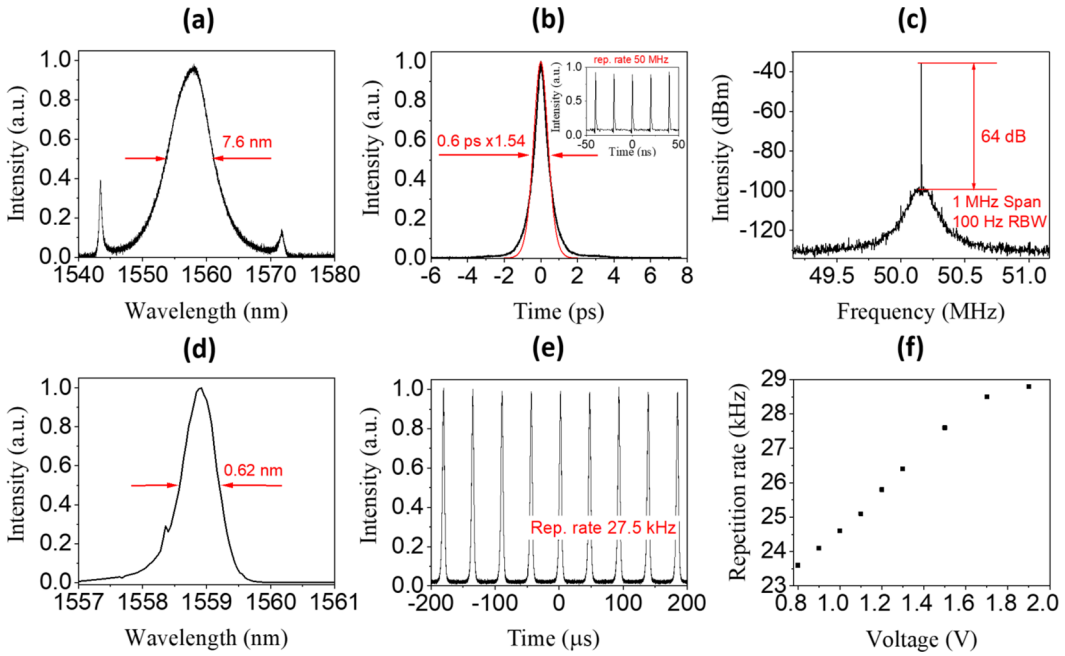

Figure 5. Top panel shows measured characteristics of ML lasing under zero gate voltage: (a) optical spectrum, (b) measured pulse autocorrelation function (black) and its theoretical fitting for the $sech^2$ shape (red) with pulse train oscillogram in the inset, and (c) RF spectrum centered at the fundamental pulse repetition frequency (RBW, resolution bandwidth). Bottom panel illustrates QS regime characteristics: (d) optical spectrum, (e) pulse train oscillogram, and (f) dependence of the pulse repetition rate on the gate voltage.

DOI: 10.1021/acs.nanolett.9b01012
Nano Lett. 2019, 19, 5836−5843

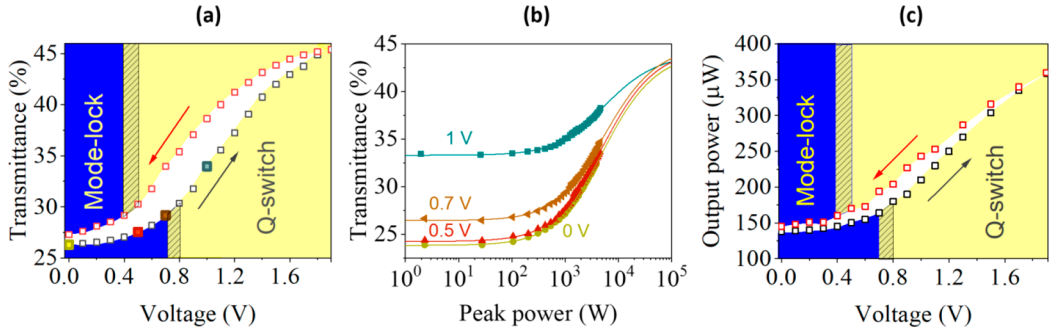

Figure 6. Maps of the gate voltage-induced switching of the laser operation between ML and QS regimes. (a) SWCNT-SA linear transmittance versus gate voltage, (b) SWCNT-SA nonlinear transmittance at different gate voltages, and (c) average output laser power versus gate voltage. The shaded regions represent the uncertainty range for the threshold voltage.

autocorrelator (see S.6 in Supporting Information for more details). Evaluation of the pulse energy from the measured average output power yields 3 pJ. The high quality of mode-locking was confirmed by the radio frequency spectrum, which featured relatively high contrast exceeding 60 dB even at high harmonics of the pulse repetition frequency (see Figure 5c and Figure S3a).

By applying a positive gate voltage to the SWCNT-SA sample we attempted to change the above ML generation regime. We continuously increased the voltage from 0 to 1.9 V. As discussed above with reference to Figures 2 and 3, the linear transmittance increases and the modulation depth of nonlinear absorption decreases under gate voltage. An increase of the gate voltage from 0 to 0.7 V resulted in a slight growth of the average output power and consequently of the pulse energy while the laser kept on single-pulse ML lasing. Above the threshold voltage of 0.7 V, the laser operation regime switched to the Q-switching. In the QS regime the laser generated microsecond pulses with a kilohertz repetition rate. Sustained QS was observed with further increase in the gate voltage up to 1.9 V. The average output power increased by a factor of 2 when the voltage was changed from 0.7 to 1.9 V. The basic laser characteristics measured in the QS regime are shown in Figure 5d–f and Figure S3b. It should be noted that by changing the gate voltage (from 0.8 to 1.9 V) the pulse repetition rate could be tuned from 23.6 to 28.8 kHz. The highest pulse energy in the QS regime reached 12.5 nJ. When the gate voltage was decreased back toward zero voltage the laser recovered the ML regime and reduced the output power in a slightly hysteretic manner (upon decreasing the threshold voltage was 0.5 V). This hysteretic behavior arises from the ionic liquid, which creates hysteresis in the voltage-induced alteration of the SWCNT-SA's optical properties. Figure 6a illustrates the measured voltage-induced variation of linear transmittance through the SWCNT-SA and the existence ranges of different pulse generation regimes. Note that the regimes get switched at the same transmittance level (and thus at the same modulation depth), irrespectively of the voltage variation direction. Fiber lasers with nearly zero anomalous dispersion require relatively high modulation depth of the saturable absorber to sustain a stable generation of ultrashort pulses.[54,55] This correlates with the observed behavior of our laser, that sustains stable mode-locking only at low gate voltages that enable high modulation depth of the SWCNT-SA.

We performed nonlinear transmittance measurements for the SWCNT-SA sample at 0, 0.5, 0.7, and 1 V, which is around the threshold voltage of pulsed regime switching. The available peak power (up to 5 kW) from the laser source used for these measurements did not allow us to fully saturate the SWCNT-SA. Fitting of the measurement data with the standard function applicable for fast saturable absorbers (solid lines in Figure 6b) allows us to retrieve the main parameters of the SA under the assumption of pure saturable absorption unaffected by other optical nonlinearities. Details on the nonlinear transmittance measurements can be found in Supporting Information (Section 7). We found that the full modulation depth reduces from 20% at 0 V to 10% at 1 V. Nevertheless, at all the indicated voltages the nonsaturable losses converge to similar values within the range of 55.5 ± 0.6% with the saturation power of 1.62 ± 0.12 kW (see Table S1). This observation supports the findings of the pump–probe section where modulation depth reduction under 1 V was attributed to excited-state filling. Figure 6c represents the variation of the laser output power measured with increasing and decreasing gate voltage. The shaded regions in Figure 6a,c represent the uncertainty range for the threshold voltage which we attribute to the inert behavior of electrochemical system under small voltage variations. The switching between the ML and QS regimes by means of the electrically gated SWCNT-SA featured a high degree of reproducibility when we swept the gate voltage across the shaded region. The speed of switching between regimes is limited by ionic diffusion in the ionic liquid. In our case, the switching time was close to a second, however, optimization of the electrochemical cell design can bring it to the millisecond time-scale.[16]

Our study expands the possibilities of the SWCNT applications in fiber lasers. Reliable lasers which allow controllable on-the-run switching of pulsed regimes can be of great benefit for material processing and medical applications, LIDAR, and 3D scanning. We note that evanescent field interaction with SWCNT-SA on the side-polished fiber demonstrates excellent thermal stability allowing pulse generation with average power exceeding hundreds of milliwatts.[56,57] It opens up possibilities for future development of high-power lasers with switchable pulsed regimes driven by the gated SWCNT-SAs. Also, the ability to tune modulation characteristics of the saturable absorber provides a useful instrument for the investigations of the pulsed laser dynamics. Moreover, this approach can be expanded on the other types of optical nonlinearities of SWCNTs including second and third harmonic generation and four wave mixing.

In summary, we have investigated the effect of electrochemical gating on the absorption saturation in SWCNT films.

DOI: 10.1021/acs.nanolett.9b01012
Nano Lett. 2019, 19, 5836–5843

With a pump−probe technique, we showed that nonlinear absorption modulation depth can be controlled by the gate voltage below 2 V. On this basis, we designed a tunable fiber-coupled saturable absorber using the gated SWCNTs deposited on a side-polished PM fiber. We implemented this device into the all-polarization-maintaining fiber laser and studied the feasibility of electrical control of the pulsed lasing regime by adjusting the gate voltage. The reproducible electrically controlled switching of the pulse generation regime between pure mode-locking (ultrashort pulses) and Q-switching (high-energy microsecond pulses) was demonstrated. Adjusting the gate voltage in the QS regime led to the fine-tuning of the output power and repetition rate. This approach opens a new avenue for carbon nanotube optical devices with tunable and scalable nonlinearity.

Materials and Methods. *Sample Fabrication.* The side-polished fibers used in the work are produced by Phoenix photonics with a panda-type polarization-maintaining fiber with polished side normal to the slow axis plane (one stress member removed). The reference silver electrode was deposited on the cover glass by thermal evaporation. The SWCNT film on the PM-SPF had a thickness of 20 nm and was 2 mm by 15 mm in size. Counter electrode of SWCNT film of the same thickness and 2 mm by 10 mm in size was offset from the working electrode by 2 mm. For ionic liquid, we used 30 μL of DEME BF_4 (*N*,*N*-diethyl-*N*-methyl-*N*-2-methoxyethylammonium tetrafluoroborate). At all the fabrication steps, we measured the transmittance through the sample with a nonpolarized Er-fiber amplified spontaneous emission (ASE) source. The transmittance of the PM-SPF dropped from 91% to 63% after SWCNTs transfer and decreases further to 45% after ionic liquid dripping. To prevent ionic liquid degradation in the presence of water vapor the sample was prepared in an argon atmosphere glovebox and sealed before removal to the air.

The sample for pump−probe measurements was made with a 40 nm thick SWCNT film and ionic gel (1-butyl-3-methylimidazolium hexafluorophosphate).

Pump−Probe Setup. A commercially available laser system (Spitfire ACE PA, Newport Spectra Physics) with 40 fs, 800 nm pulse at 1 kHz repetition rate was used to pump two OPA systems (TOPAS, Light Conversion). Each TOPAS was tuned to 1540 nm resulting in a degenerate pump−probe scheme. To avoid interference, the pump and probe beams were cross-polarized. The probe pulse was focused into the sample with the pump pulse being focused in a near collinear arrangement with some distance behind the sample to ensure the pump beam is always at least three times the size of the probe beam. Prior to this, the probe beam is split 50:50 to produce a probe and a reference beam. The pump and probe fluences were 382 and 159 $\mu J\ cm^{-2}$, respectively, each controlled by a variable reflective neutral density filter. The working spectral width was 50 nm (full width at 10% of spectral amplitude) around the 1540 nm central wavelength. The probe light was analyzed after the sample using an imaging spectrometer (iHR320, Horiba) and measured using a liquid N_2 cooled mercury cadmium telluride detector with two arrays of 64 pixels, allowing a spectral window of 50 nm to be measured with each pixel corresponding to a 1.3 nm wavelength range. Data in the main text are presented for the pixel at 1540 nm. The scattered pump light on the detector was minimized using an iris aperture to block the transmitted pump beam and pass the probe. The probe and reference beams are each focused onto one of the two arrays. This allows the signal to be normalized for shot-to-shot variations in power.

Pulsed Laser Measurements. Measurements of the fiber laser pulse generation were performed with a Newport 818-BB-35F photodetector having 12 GHz bandwidth and 25 ps rise time, a Tektronix DPO 7254 oscilloscope with 2.5 GHz bandwidth, a Tektronix RSA 3308B radio frequency spectrum analyzer, a Yokogawa AQ 6375 optical spectrum analyzer with 0.02 nm resolution, an APE pulseCheck autocorrelator with a scanning range from 120 fs up to 150 ps, and a Thorlabs PM100D power meter with S132C photodiode power sensor heads.

■ ASSOCIATED CONTENT

Supporting Information

The Supporting Information is available free of charge on the ACS Publications website at DOI: 10.1021/acs.nanolett.9b01012.

Animation of sample fabrication (AVI)

Cyclic voltammetry and full spectra of the carbon nanotubes, details on autocorrelation and nonlinear transmittance measurements and as well as details on voltage-induced switching of pulse lasing regimes in an alternative fiber laser scheme based on single-mode fibers without polarization maintaining (PDF)

■ AUTHOR INFORMATION

Corresponding Authors

*E-mail: y.gladush@skoltech.ru.
*E-mail: a.nasibulin@skoltech.ru.

ORCID

Yuriy Gladush: 0000-0002-1289-2654
Aram A. Mkrtchyan: 0000-0002-6610-6006
Daria S. Kopylova: 0000-0002-8685-7966
Boris Nyushkov: 0000-0002-3913-1230
James Lloyd-Hughes: 0000-0002-9680-0138
Albert G. Nasibulin: 0000-0002-1684-3948

Notes

The authors declare no competing financial interest.

■ ACKNOWLEDGMENTS

Authors thank Prof. Galina Tsirlina and Dr. Victioria Nikitina for valuable discussion on the ionic liquid gating. Y.G., A.A.M., D.S.K., and A.G.N. thank the Russian Science Foundation (No. 17-19-01787) for support of the work on SWCNT synthesis and electrochemical doping. The U.K. authors would like to thank the ESPRC for support of this work under Grant EP/N010825/1. A.I. thanks the RFBR for support of his laser part of the work under Grant 18-32-20021.

■ REFERENCES

(1) Maiti, U. N.; Lee, W. J.; Lee, J. M.; Oh, Y.; Kim, J. Y.; Kim, J. E.; Shim, J.; Han, T. H.; Kim, S. O. 25th Anniversary Article: Chemically Modified/Doped Carbon Nanotubes & Graphene for Optimized Nanostructures & Nanodevices. *Adv. Mater.* **2014**, *26* (1), 40−67.

(2) Duclaux, L. Review of the Doping of Carbon Nanotubes (Multiwalled and Single-Walled). *Carbon* **2002**, *40*, 1751−1764.

(3) Kazaoui, S.; Minami, N.; Jacquemin, R.; Kataura, H.; Achiba, Y. Amphoteric Doping of Single-Wall Carbon-Nanotube Thin Films as Probed by Optical Absorption Spectroscopy. *Phys. Rev. B: Condens. Matter Mater. Phys.* **1999**, *60* (19), 13339−13342.

DOI: 10.1021/acs.nanolett.9b01012
Nano Lett. 2019, 19, 5836−5843

(4) Kazaoui, S.; Minami, N.; Matsuda, N.; Kataura, H.; Achiba, Y. Electrochemical Tuning of Electronic States in Single-Wall Carbon Nanotubes Studied by in Situ Absorption Spectroscopy and Ac Resistance. *Appl. Phys. Lett.* **2001**, *78* (22), 3433−3435.
(5) Wu, Z.; Wu, Z.; Chen, Z.; Du, X.; Logan, J. M.; Sippel, J.; Nikolou, M.; Kamaras, K.; Reynolds, J. R.; Tanner, D. B. Transparent, Conductive Carbon Nanotube Films. *Science* **2004**, *305* (5688), 1273−1276.
(6) Bisri, S. Z.; Shimizu, S.; Nakano, M.; Iwasa, Y. Endeavor of Iontronics : From Fundamentals to Applications of Ion-Controlled Electronics. *Adv. Mater.* **2017**, *29*, 1607054−1607054.
(7) Park, J. S.; Hirana, Y.; Mouri, S.; Miyauchi, Y.; Nakashima, N.; Matsuda, K. Observation of Negative and Positive Trions in the Electrochemically Carrier-Doped Single-Walled Carbon Nanotubes. *J. Am. Chem. Soc.* **2012**, *134* (35), 14461−14466.
(8) Eckstein, K. H.; Hartleb, H.; Achsnich, M. M.; Schöppler, F.; Hertel, T. Localized Charges Control Exciton Energetics and Energy Dissipation in Doped Carbon Nanotubes. *ACS Nano* **2017**, *11* (10), 10401−10408.
(9) Möhl, C.; Graf, A.; Berger, F. J.; Lüttgens, J.; Zakharko, Y.; Lumsargis, V.; Gather, M. C.; Zaumseil, J. Trion-Polariton Formation in Single-Walled Carbon Nanotube Microcavities. *ACS Photonics* **2018**, *5* (6), 2074−2080.
(10) Burdanova, M. G.; Tsapenko, A. P.; Satco, D. A.; Kashtiban, R. J.; Mosley, C. D. W.; Monti, M.; Staniforth, M.; Sloan, J.; Gladush, Y. G.; Nasibulin, A. G.; et al. Giant Negative Terahertz Photoconductivity in Controllably Doped Carbon Nanotube Networks. *ACS Photonics* **2019**, *6* (4), 1058−1066.
(11) Igarashi, T.; Kawai, H.; Yanagi, K.; Cuong, N. T.; Okada, S.; Pichler, T. Tuning Localized Transverse Surface Plasmon Resonance in Electricity-Selected Single-Wall Carbon Nanotubes by Electrochemical Doping. *Phys. Rev. Lett.* **2015**, *114* (17), 176807.
(12) Yanagi, K.; Okada, R.; Ichinose, Y.; Yomogida, Y.; Katsutani, F.; Gao, W.; Kono, J. Intersubband Plasmons in the Quantum Limit in Gated and Aligned Carbon Nanotubes. *Nat. Commun.* **2018**, *9* (1), 1121.
(13) Yanagi, K.; Moriya, R.; Yomogida, Y.; Takenobu, T.; Naitoh, Y.; Ishida, T.; Kataura, H.; Matsuda, K.; Maniwa, Y. Electrochromic Carbon Electrodes: Controllable Visible Color Changes in Metallic Single-Wall Carbon Nanotubes. *Adv. Mater.* **2011**, *23* (25), 2811−2814.
(14) Wang, F.; Itkis, M. E.; Bekyarova, E.; Haddon, R. C. Charge-Compensated, Semiconducting Single-Walled Carbon Nanotube Thin Film as an Electrically Configurable Optical Medium. *Nat. Photonics* **2013**, *7* (6), 459−465.
(15) Berger, F. J.; Higgins, T. M.; Rother, M.; Graf, A.; Zakharko, Y.; Allard, S.; Matthiesen, M.; Gotthardt, J. M.; Scherf, U.; Zaumseil, J. From Broadband to Electrochromic Notch Filters with Printed Monochiral Carbon Nanotubes. *ACS Appl. Mater. Interfaces* **2018**, *10* (13), 11135−11142.
(16) Moser, M. L.; Li, G.; Chen, M.; Bekyarova, E.; Itkis, M. E.; Haddon, R. C. Fast Electrochromic Device Based on Single-Walled Carbon Nanotube Thin Films. *Nano Lett.* **2016**, *16* (9), 5386−5393.
(17) Mishra, S. R.; Rawat, H. S.; Mehendale, S. C.; Rustagi, K. C.; Sood, A. K.; Bandyopadhyay, R.; Govindaraj, A.; Rao, C. N. R. Optical Limiting in Single-Walled Carbon Nanotube Suspensions. *Chem. Phys. Lett.* **2000**, *317* (3−5), 510−514.
(18) Ní Mhuircheartaigh, É. M.; Giordani, S.; Blau, W. J. Linear and Nonlinear Optical Characterization of a Tetraphenylporphyrin−Carbon Nanotube Composite System. *J. Phys. Chem. B* **2006**, *110* (46), 23136−23141.
(19) Wang, J.; Chen, Y.; Blau, W. J. Carbon Nanotubes and Nanotube Composites for Nonlinear Optical Devices. *J. Mater. Chem.* **2009**, *19* (40), 7425−7443.
(20) De Dominicis, L.; Botti, S.; Asilyan, L. S.; Ciardi, R.; Fantoni, R.; Terranova, M. L.; Fiori, A.; Orlanducci, S.; Appolloni, R. Second- and Third-Harmonic Generation in Single-Walled Carbon Nanotubes at Nanosecond Time Scale. *Appl. Phys. Lett.* **2004**, *85* (8), 1418−1420.
(21) Huttunen, M. J.; Herranen, O.; Johansson, A.; Jiang, H.; Mudimela, P. R.; Myllyperkiö, P.; Bautista, G.; Nasibulin, A. G.; Kauppinen, E. I.; Ahlskog, M.; et al. Measurement of Optical Second-Harmonic Generation from an Individual Single-Walled Carbon Nanotube. *New J. Phys.* **2013**, *15*, 083043.
(22) Chow, K. K.; Yamashita, S. Four-Wave Mixing in a Single-Walled Carbon-Nanotube-Deposited D-Shaped Fiber and Its Application in Tunable Wavelength Conversion. *Opt. Express* **2009**, *17* (18), 15608−15613.
(23) Kim, H.; Kim, H.; Sheps, T.; Sheps, T.; Collins, P. G.; Collins, P. G.; Potma, E. O.; Potma, E. O. Nonlinear Optical Imaging of Individual Carbon Nanotubes with Four-Wave-Mixing Microscopy. *Nano Lett.* **2009**, *9* (8), 2991.
(24) Lee, K. F.; Tian, Y.; Yang, H.; Mustonen, K.; Martinez, A.; Dai, Q.; Kauppinen, E. I.; Malowicki, J.; Kumar, P.; Sun, Z. Photon-Pair Generation with a 100 Nm Thick Carbon Nanotube Film. *Adv. Mater.* **2017**, *29* (24), 1605978.
(25) Myllyperkio, P.; Herranen, O.; Rintala, J.; Jiang, H.; Mudimela, P. R.; Zhu, Z.; Nasibulin, A. G.; Johansson, A.; Kauppinen, E. I.; Ahlskog, M. Femtosecond Four-Wave-Mixing Spectroscopy of Suspended Individual Semiconducting Single-Walled Carbon Nanotubes. *ACS Nano* **2010**, *4* (11), 6780−6786.
(26) Maeda, A.; Matsumoto, S.; Kishida, H.; Takenobu, T.; Iwasa, Y.; Shiraishi, M.; Ata, M.; Okamoto, H. Large Optical Nonlinearity of Semiconducting Single-Walled Carbon Nanotubes under Resonant Excitations. *Phys. Rev. Lett.* **2005**, *94* (4), 047404.
(27) Xu, S.; Wang, F.; Zhu, C.; Meng, Y.; Liu, Y.; Liu, W.; Tang, J.; Liu, K.; Hu, G.; Howe, R. C. T.; et al. Ultrafast Nonlinear Photoresponse of Single-Wall Carbon Nanotubes: A Broadband Degenerate Investigation. *Nanoscale* **2016**, *8* (17), 9304−9309.
(28) Hasan, T.; Sun, Z.; Wang, F.; Bonaccorso, F.; Tan, P. H.; Rozhin, A. G.; Ferrari, A. C. Nanotube - Polymer Composites for Ultrafast Photonics. *Adv. Mater.* **2009**, *21* (38−39), 3874−3899.
(29) Kivistö, S.; Hakulinen, T.; Kaskela, A.; Aitchison, B.; Brown, D. P.; Nasibulin, A. G.; Kauppinen, E. I.; Härkönen, A.; Okhotnikov, O. G. Carbon Nanotube Films for Ultrafast Broadband Technology. *Opt. Express* **2009**, *17* (4), 2358.
(30) Set, S. Y.; Yaguchi, H.; Tanaka, Y.; Jablonski, M. Ultrafast Fiber Pulsed Lasers Incorporating Carbon Nanotubes. *IEEE J. Sel. Top. Quantum Electron.* **2004**, *10* (1), 137−146.
(31) Wang, F.; Rozhin, A. G.; Scardaci, V.; Sun, Z.; Hennrich, F.; White, I. H.; Milne, W. I.; Ferrari, A. C. Wideband-Tuneable, Nanotube Mode-Locked, Fibre Laser. *Nat. Nanotechnol.* **2008**, *3* (12), 738−742.
(32) Chernysheva, M.; Rozhin, A.; Fedotov, Y.; Mou, C.; Arif, R.; Kobtsev, S. M.; Dianov, E. M.; Turitsyn, S. K. Carbon Nanotubes for Ultrafast Fibre Lasers. *Nanophotonics* **2017**, *6* (1), 1−30.
(33) Im, J. H.; Choi, S. Y.; Rotermund, F.; Yeom, D.-I. All-Fiber Er-Doped Dissipative Soliton Laser Based on Evanescent Field Interaction with Carbon Nanotube Saturable Absorber. *Opt. Express* **2010**, *18* (21), 22141−22146.
(34) Sobon, G.; Duzynska, A.; Świniarski, M.; Judek, J.; Sotor, J.; Zdrojek, M. CNT-Based Saturable Absorbers with Scalable Modulation Depth for Thulium-Doped Fiber Lasers Operating at 1.9 Mm. *Sci. Rep.* **2017**, *7*, 45491.
(35) Li, D.; Xue, H.; Qi, M.; Wang, Y.; Aksimsek, S.; Chekurov, N.; Kim, W.; Li, C.; Riikonen, J.; Ye, F.; et al. Graphene Actively Q-Switched Lasers. *2D Mater.* **2017**, *4* (2), 025095.
(36) Bogusławski, J.; Wang, Y.; Xue, H.; Yang, X.; Mao, D.; Gan, X.; Ren, Z.; Zhao, J.; Dai, Q.; Soboń, G.; et al. Graphene Actively Mode-Locked Lasers. *Adv. Funct. Mater.* **2018**, *28*, 1801539.
(37) Lee, E. J.; Choi, S. Y.; Jeong, H.; Park, N. H.; Yim, W.; Kim, M. H.; Park, J. K.; Son, S.; Bae, S.; Kim, S. J.; et al. Active Control of All-Fibre Graphene Devices with Electrical Gating. *Nat. Commun.* **2015**, *6*, 6851.
(38) Alexander, K.; Savostianova, N. A.; Mikhailov, S. A.; Kuyken, B.; Van Thourhout, D. Electrically Tunable Optical Nonlinearities in Graphene-Covered SiN Waveguides Characterized by Four-Wave Mixing. *ACS Photonics* **2017**, *4* (12), 3039−3044.

DOI: 10.1021/acs.nanolett.9b01012
Nano Lett. 2019, 19, 5836−5843

(39) Jiang, T.; Huang, D.; Cheng, J.; Fan, X.; Zhang, Z.; Shan, Y.; Yi, Y.; Dai, Y.; Shi, L.; Liu, K.; et al. Gate-Tunable Third-Order Nonlinear Optical Response of Massless Dirac Fermions in Graphene. *Nat. Photonics* **2018**, *12*, 430−437.
(40) Soavi, G.; Wang, G.; Rostami, H.; Purdie, D. G.; De Fazio, D.; Ma, T.; Luo, B.; Wang, J.; Ott, A. K.; Yoon, D.; et al. Broadband, Electrically Tunable Third-Harmonic Generation in Graphene. *Nat. Nanotechnol.* **2018**, *13* (7), 583−588.
(41) Wu, J.; Tang, D. Y.; Zhao, L. M.; Chan, C. C. Soliton Polarization Dynamics in Fiber Lasers Passively Mode-Locked by the Nonlinear Polarization Rotation Technique. *Phys. Rev. E - Stat. Nonlinear, Soft Matter Phys.* **2006**, *74* (4), 046605.
(42) Tian, Y.; Nasibulin, A. G.; Aitchison, B.; Nikitin, T.; Pfaler, J. V.; Jiang, H.; Zhu, Z.; Khriachtchev, L.; Brown, D. P.; Kauppinen, E. I. Controlled Synthesis of Single-Walled Carbon Nanotubes in an Aerosol Reactor. *J. Phys. Chem. C* **2011**, *115* (15), 7309−7318.
(43) Tian, Y.; Timmermans, M. Y.; Kivistö, S.; Nasibulin, A. G.; Zhu, Z.; Jiang, H.; Okhotnikov, O. G.; Kauppinen, E. I. Tailoring the Diameter of Single-Walled Carbon Nanotubes for Optical Applications. *Nano Res.* **2011**, *4* (8), 807−815.
(44) Mikheev, G. M.; Nasibulin, A. G.; Zonov, R. G.; Kaskela, A.; Kauppinen, E. I. Photon-Drag Effect in Single-Walled Carbon Nanotube Films. *Nano Lett.* **2012**, *12*, 77−83.
(45) Kaskela, A.; Nasibulin, A. G.; Timmermans, M. Y.; Aitchison, B.; Papadimitratos, A.; Tian, Y.; Zhu, Z.; Jiang, H.; Brown, D. P.; Zakhidov, A.; et al. Aerosol-Synthesized SWCNT Networks with Tunable Conductivity and Transparency by a Dry Transfer Technique. *Nano Lett.* **2010**, *10* (11), 4349−4355.
(46) Korovyanko, O. J.; Sheng, C. X.; Vardeny, Z. V.; Dalton, A. B.; Baughman, R. H. Ultrafast Spectroscopy of Excitons in Single-Walled Carbon Nanotubes. *Phys. Rev. Lett.* **2004**, *92* (1), 017403.
(47) Nishihara, T.; Yamada, Y.; Kanemitsu, Y. Dynamics of Exciton-Hole Recombination in Hole-Doped Single-Walled Carbon Nanotubes. *Phys. Rev. B: Condens. Matter Mater. Phys.* **2012**, *86* (7), 075449.
(48) Haus, H. A. Parameter Ranges for CW Passive Mode Locking. *IEEE J. Quantum Electron.* **1976**, *12* (3), 169−176.
(49) Namiki, S.; Ippen, E. P.; Haus, H. a.; Yu, C. X. Energy Rate Equations for Mode-Locked Lasers. *J. Opt. Soc. Am. B* **1997**, *14* (8), 2099.
(50) Honninger, C.; Paschotta, R.; Morier-Genoud, F.; Moser, M.; Keller, U. Q -Switching Stability Limits of Continuous-Wave Passive Mode Locking. *J. Opt. Soc. Am. B* **1999**, *16* (1), 46−56.
(51) Gene, J.; Park, N. H.; Jeong, H.; Choi, S. Y.; Rotermund, F.; Yeom, D.-I.; Kim, B. Y. Optically Controlled In-Line Graphene Saturable Absorber for the Manipulation of Pulsed Fiber Laser Operation. *Opt. Express* **2016**, *24* (19), 21301.
(52) Lin, K.-H.; Kang, J.-J.; Wu, H.-H.; Lee, C.-K.; Lin, G.-R. Manipulation of Operation States by Polarization Control in an Erbium-Doped Fiber Laser with a Hybrid Saturable Absorber. *Opt. Express* **2009**, *17* (6), 4806−4814.
(53) Nelson, L. E.; Jones, D. J.; Tamura, K.; Haus, H. A.; Ippen, E. P. Ultrashort-Pulse Fiber Ring Lasers. *Appl. Phys. B: Lasers Opt.* **1997**, *65* (2), 277−294.
(54) Liu, H. H.; Chow, K. K. Enhanced Stability of Dispersion-Managed Mode-Locked Fiber Lasers with near-Zero Net Cavity Dispersion by High-Contrast Saturable Absorbers. *Opt. Lett.* **2014**, *39* (1), 150.
(55) Jeon, J.; Lee, J.; Lee, J. H. Numerical Study on the Minimum Modulation Depth of a Saturable Absorber for Stable Fiber Laser Mode Locking. *J. Opt. Soc. Am. B* **2015**, *32* (1), 31.
(56) Liu, H. H.; Chow, K. K.; Yamashita, S.; Set, S. Y. Carbon-Nanotube-Based Passively Q-Switched Fiber Laser for High Energy Pulse Generation. *Opt. Laser Technol.* **2013**, *45* (1), 713−716.
(57) Mkrtchyan, A. A.; Gladush, Y. G.; Galiakhmetova, D.; Yakovlev, V.; Ahtyamov, V. T.; Nasibulin, A. G. Dry-Transfer Technique for Polymer-Free Single-Walled Carbon Nanotube Saturable Absorber on a Side Polished Fiber. *Opt. Mater. Express* **2019**, *9* (4), 1551.

DOI: 10.1021/acs.nanolett.9b01012
Nano Lett. 2019, 19, 5836−5843